Extreme Mechanics Letters 41 (2020) 101013

Contents lists available at ScienceDirect

Extreme Mechanics Letters

journal homepage: www.elsevier.com/locate/eml

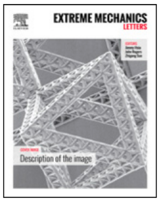

# Generalized rate-and-state model linking rheology and soft matter tribology

Jiho Kim [a], Alison C. Dunn [b,*]

[a] University of Florida, Department of Mechanical and Aerospace Engineering, Gainesville, FL 32611, United States of America
[b] University of Illinois at Urbana-Champaign, Department of Mechanical Science and Engineering, Urbana, IL 61801, United States of America

## ARTICLE INFO

*Article history:*
Received 10 July 2020
Received in revised form 2 September 2020
Accepted 28 September 2020
Available online 30 September 2020

*Keywords:*
Thixotropy
Hydrogel lubrication
Rate-and-state friction model

## ABSTRACT

In the present work, a complex fluid lubrication model based on a single state variable named the structural parameter was used to predict steady-state frictional responses for a continuous hydrogel-on-flat contact. The model predicts the steady-state lubrication curve, or steady-state friction versus sliding speed curve, that was only previously predicted by the adsorption friction model, a widely used model for hydrogel lubrication. For the first time, model can predict the analytical solutions of two transition speeds in the steady-state lubrication curve rather than the single critical speed in the adsorption model. Finally, we suggest a physical meaning of the structural parameter based on a comparison with the rate-and-state friction model used for geological events. We posit that it is measure of real contact area mediated by the water intervention. This is the first study to connect various fields including rheology, soft matter tribology, and geological physics.

## 1. Introduction

In recent decades, there have been many efforts to discover a lubrication curve which shows the relationship between friction and speed for soft hydrated gels in sliding, and several mechanics and materials models were suggested to describe the shape of the curves [1–6]. One of the most widely used model is the repulsion–adsorption model by Gong [1,7–9]. Following Schallamach's approach for rubber friction [10], the adsorption model was formulated to predict the shape of the steady-state friction versus sliding speed curve using computational simulation [1]. Gong assembled the lubrication curve, or friction versus speed curve, for hydrogels based on the steady-state frictional response at particular sliding speeds in a rheometer, reporting that there is a transient response in each speed [7]. The model generally explains the shape of steady-state lubrication curve and provides the description of mechanisms in different lubrication regimes based on polymer physics. However, because the transient response is not considered in the model, it can only describe the steady-state response. In practical applications, short-time friction may be important, and as such a complete lubrication model must include it.

While most hydrogel lubrication studies assume a steady state of sliding, our prior study discovered that under constant sliding, the friction of a hydrogel interface was influenced strongly by the history of sliding to that point [11]. That transient lubrication led to a hysteretic lubrication curve when increasing or decreasing sliding speed. The study assumed that 90 s sliding duration was sufficiently long to represent a steady-state condition, but it had no theoretical support. In a follow-up study, computation-based simulations accurately reproduced the hysteresis shapes measured under the various sliding durations used in the experiments. These simulations modeled the transient friction as shear of a thixotropic fluid [12].

In this letter, we identify a more refined form of the complex fluid lubrication model and verify that the model predicts the steady-state response previously reported by Gong [7]. Based on the similarity between the complex fluid lubrication model and rate-and-state friction model, we suggest the physical mechanism that drives the transient mechanics of hydrogel lubrication.

## 2. Experimental data for modeling

For the curve fitting and simulation, the same experimental data that was presented in the previous study is used [12]. In the prior study, the sliding test was conducted in a tribo-rheometry setup resembling a thrust washer tribometer to induce unidirectional continuous sliding. The change of sliding speed input was done in a stepwise manner, and frictional torque output was measured at each sliding speed. The controlling factor that determined hysteresis shape of lubrication curves was the duration of sliding at each step, and 5 different durations were used for experiment and model fitting in the prior study. The same model

---

* Corresponding author.
*E-mail address:* acd@illinois.edu (A.C. Dunn).

https://doi.org/10.1016/j.eml.2020.101013

fitting and simulation are conducted in the current study with a simplified and refined model for broader applicability.

## 3. Modeling and simulation methods

### 3.1. Complex fluid lubrication model

Complex fluid lubrication models are composed of two main relations: the first is the product of viscosity and shear rate as a shear stress, where viscosity can be a function of a state variable called the structural parameter $\lambda$ [12]. The second relation describes the change of the state variable with time as a function of its current value and the driving velocity $V$. In the prior work, we used power law fluid model as the first relation to describe the power law relation found in the experiment. However, in the present study, we follow established hydrogel lubrication studies that interpreted the power law relation between friction and sliding speed as a Newtonian fluid flow with changing gap height [5,8,13–15]. We reformulate the first relation into Eq. (1).

$$\tau = \eta(\lambda)\dot{\gamma} = \eta(\lambda)\frac{V}{h(V)}, \qquad where\ \eta(\lambda) = \eta_s + \lambda\eta_p\ ,\ \ h(V) = CV^{1-\alpha}\ , \tag{1}$$

In Eq. (1), $\tau$ is a fluid shear stress under sliding, $\eta_s$ is the water viscosity, $\eta_p$ is a viscosity coefficient of the structural parameter $\lambda$, $\dot{\gamma}$ is a shear rate, $V$ is a linear sliding speed, and $h$ is an effective gap height, $\alpha$ is the power law exponent found in lubrication curves at the high speed regime [12], and $C$ is a constant with a dimension of $[L^\alpha T^{1-\alpha}]$, where $L$ is length and $T$ is time.

The benefit of allowing variable gap height rather than a constant of 100 nm in the prior work is that we can assign the known viscosity value of water and calculate the gap height value. The gap height calculated based on the new model ranges from 32 to 248 nm depending on the sliding speed.

Shear stress $\tau$ is also a function of structural parameter $\lambda$, which is predicted by a kinetic equation

$$\frac{d\lambda}{dt} = -k_1\frac{V}{V_{\max}}\lambda^a + k_2\left(1-\lambda\right)^b , \tag{2}$$

where $k_1$ and $k_2$ are rate coefficients, $a$ and $b$ are power law exponents that determine the dependence of each rate term to $\lambda$, and $V/V_{max}$ is a normalized sliding speed. The changing $\lambda$ over time obtained by solving the differential equation closely simulates the transient frictional behavior and lubrication hysteresis [12].

### 3.2. Lubrication hysteresis simulation

The modification of the model does not affect the curve fitting accuracy because it does not change the overall form of equations; rather, it just scales each parameter in the fitting results. The scaled model constants for the modified model are tabulated in Table 1. Using the new model and model constants, hysteresis curves at 5 different step times from 9 to 90 s are simulated by solving differential equation Eq. (2). The input of the simulation is the sliding speed, which initially decreases stepwise from 50 to 0.05 rad/s through 16 steps and returning to the highest speed with the same number of steps. Finite difference method is used to solve the differential equation with initial value of $\lambda = 0$ at the highest speed. This gives the shear stress or friction response over time. The last friction value at each step is used as representative force at each sliding speed.

### 3.3. Steady-state lubrication simulation

Assuming that the complex model applies for longer sliding durations than the step times used in the previous study [12], we simulated for the steady-state response of the complex lubrication. The step time, or the duration at each step, is increased until the lubrication curves ceases to change.

**Table 1**
The scaled fitting parameters for the modified model.

| $\alpha$ | $C$ ($m^{0.7}$ $s^{0.3}$) | $\eta_p$ (Pa-s) | $k_1$ | $k_2$ | $a$ | $b$ |
|---|---|---|---|---|---|---|
| 0.7 | 2.52E−7 | 0.0118 | 0.0353 | 1.19E−3 | 0.249 | 0.701 |

## 4. Results of the simulation

The result of lubrication hysteresis and steady-state simulations are plotted in frictional torque vs. sliding angular speed to match the variables used in the tribo-rheometery experiment (Fig. 1A). Unlike the initial trend that longer step duration causes greater hysteresis at shorter step times, the hysteresis area decreases when step time increases, and finally converges to a single curve. If the frictional torque is plotted continuously over time, we observe the opposite direction of friction change depending on the direction of the speed changes (Fig. 1B). The steady-state response occurred when step time is greater than 2000 s. The step time of the steady state in Fig. 1 is 5061 s.

Gong previously reported the steady-state lubrication curve for hydrogels [7]. In her experiment, the duration of sliding was 3600 s, which is greater than the steady-state time scale from the simulation. The shape of the steady-state curve from the simulation closely matches to the shape of the lubrication curve reported by Gong, which shows that the complex fluid lubrication model well predicts the steady-state response. Based on this result, we acknowledge that the steady-state assumption that was made in our first study [11] about the hydrogel lubrication hysteresis with step time below 90 s was inappropriate, and much longer sliding duration is required to reach the steady state.

## 5. Analytic solution of critical speeds

Gong explains the shape of the curve using an adsorption model [7,9]. The model predicts the critical sliding speed (local maximum) using single-chain polymer mechanics (Fig. 2A). The critical speed is not an analytic solution, but an estimated expression derived from a scaling law.

On the other hand, the complex fluid lubrication model can provide analytical solutions of multiple critical sliding speeds. In the steady state, the change of lambda vanishes to zero (Eq. (3)), leaving a relation between the dimensionless velocity and the steady-state structural parameter (Eq. (4)).

$$\frac{d\lambda}{dt} = 0 = -k_1\frac{V}{V_{\max}}\lambda_{ss}^a + k_2\left(1-\lambda_{ss}\right)^b \tag{3}$$

$$\rightarrow \frac{V}{V_{\max}} = \frac{k_2\left(1-\lambda_{ss}\right)^b}{k_1\lambda_{ss}^a} \tag{4}$$

If Eq. (4) is solved for $\lambda_{ss}$, $\lambda_{ss}$ will be some function of sliding speed. Therefore, the steady-state frictional shear stress $\tau_{ss}$

$$\tau_{ss} = (\eta_s + \lambda_{ss}\eta_p)\frac{V^\alpha}{C} \tag{5}$$

will be a function of the sliding speed $V$ as well. Even though it is hard to express the shear stress in terms of sliding speed in an analytical form, we can still analytically solve for critical points where the slope of the shear stress versus sliding speed curve becomes zero. If we differentiate Eq. (5) with respect to $V$, and set it to zero, we get the condition for local maximum and minimum points in the steady-state lubrication curve.

$$\frac{\partial\tau_{ss}}{\partial V} = \frac{\partial\lambda_{ss}}{\partial V}\eta_p\frac{V^\alpha}{C} + \left(\eta_s + \lambda_{ss}\eta_p\right)\alpha\frac{V^{\alpha-1}}{C} = 0 \tag{6}$$

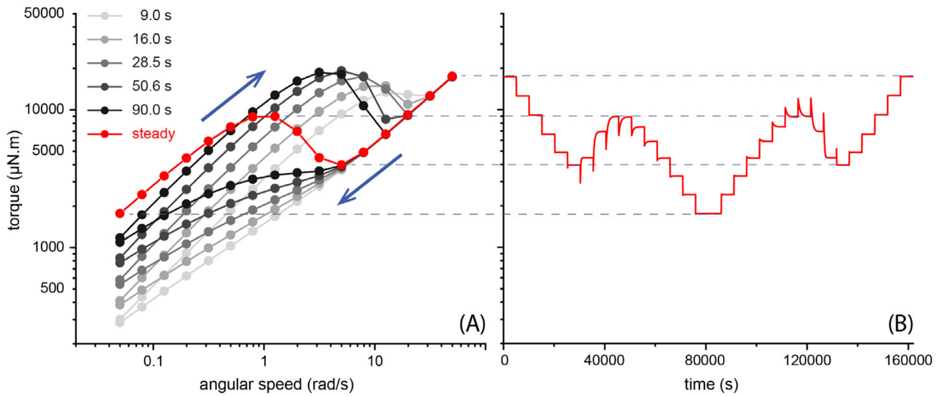

**Fig. 1.** (A) Steady state response (step time of 5061 s) of the complex fluid lubrication model plotted together with the other hysteresis curves. The different curves at increasing and decreasing speeds converge to one curve. The shape of the steady state response is identical with the representative shape of the lubrication curve for adsorptive friction [9]. (B) Frictional torque vs. time plot of the steady-state response. The friction converges to the same value at each speed, even though the direction of the transient change in each step is opposite depending on the direction of speed change.

Further, the expression for $\partial\lambda_{ss}/\partial V$ is obtained by differentiating Eq. (3).

$$\frac{\partial\lambda_{ss}}{\partial V} = \left\{\frac{-\left(1-\lambda_{ss}\right)\lambda_{ss}}{a\left(1-\lambda_{ss}\right)+b\lambda_{ss}}\right\}\frac{1}{V} \tag{7}$$

By rearranging Eq. (6) after substituting Eq. (7), we can get a quadratic equation of the structure values that correspond to the local extrema at nonzero speeds.

$$\begin{aligned} &X\lambda_{ss}^2 + Y\lambda_{ss} + Z = 0,\\ &\text{where } X = -\left(a\alpha-1\right)\eta_p + b\alpha\eta_p\\ &\qquad\quad Y = -a\alpha\eta_s + \left(a\alpha-1\right)\eta_p + b\alpha\eta_s\\ &\qquad\quad Z = a\alpha\eta_s \end{aligned} \tag{8}$$

If solved for $\lambda_{ss}$, it gives two solutions $\lambda_1$ and $\lambda_2$ that are structure parameter values corresponding to the two extrema in the lubrication curve. The solutions are substituted into Eq. (4) to get critical sliding speeds $V_1$ and $V_2$ and converted into angular speeds, which are two critical speeds showing slope transition.

$$V_{1,2} = \frac{k_2\left(1-\lambda_{1,2}\right)^b}{k_1\lambda_{1,2}^a}V_{\max}, \tag{9}$$

$$\omega_{1,2} = \frac{2}{r_o+r_i}V_{1,2} \tag{10}$$

Using the constant values found from curve fitting (Table 1), the angular speeds $\omega_1$ and $\omega_2$ are calculated: 1.03 and 4.45 rad/s, respectively. The values are plotted together with the steady state curve in Fig. 2B.

The complex fluid lubrication model not only predicts the local maximum speed but also predicts the local minimum speed in analytical form. The prediction of the second transition speed is important because it is of interest of many recent studies about hydrogel friction [3,6,16,17]. The studies found a transition from constant or slightly negative slope of friction to hydrodynamic-like regime that follows a power law. The negative slope will be discussed more in next section. Since all of these studies use sphere-on-flat geometry for the sliding, where friction reaches to the steady state quickly due to low contact area compared to the tribo-rheometry setup, there is a possibility that the steady-state response of the complex fluid lubrication model can be applied to those results. In this case, the second transition point correspond to the transition points found in those studies based on the shape of the curve.

However, unlike the adsorption model, the complex fluid lubrication model does not provide the physical interpretation of the transition speed and lubrication regimes. Another friction model, the *rate-and-state* model, has never been considered for application to hydrogel lubrication, but can give a critical insight on the physical meaning of complex, fluid-like hydrogel lubrication.

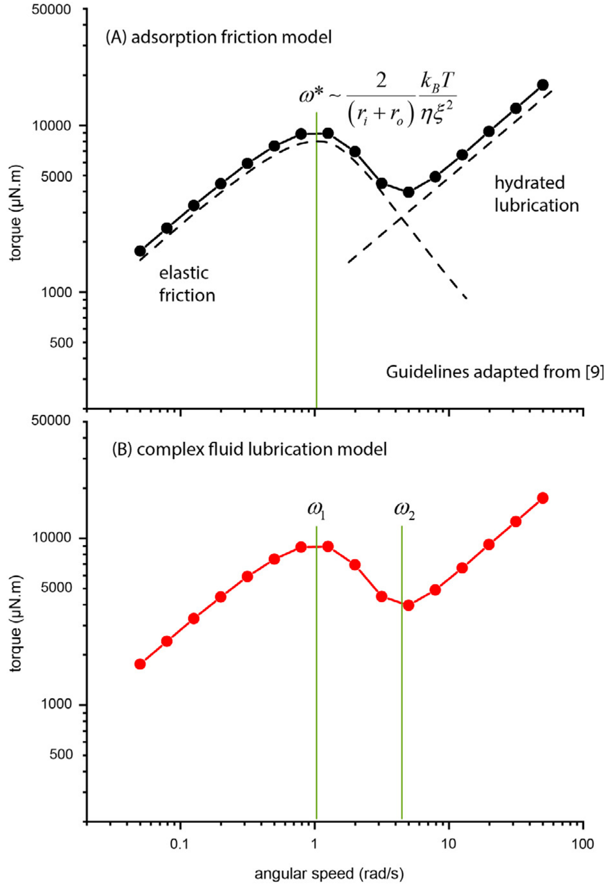

**Fig. 2.** The comparison between the steady state curve of the complex fluid lubrication model and the adsorption model. The transition points found in the complex fluid lubrication model are analytical solutions directly derived from equations, while the transition point of adsorption model is derived conceptually using scaling law to explain the transition point found in the computational calculation [7,9].

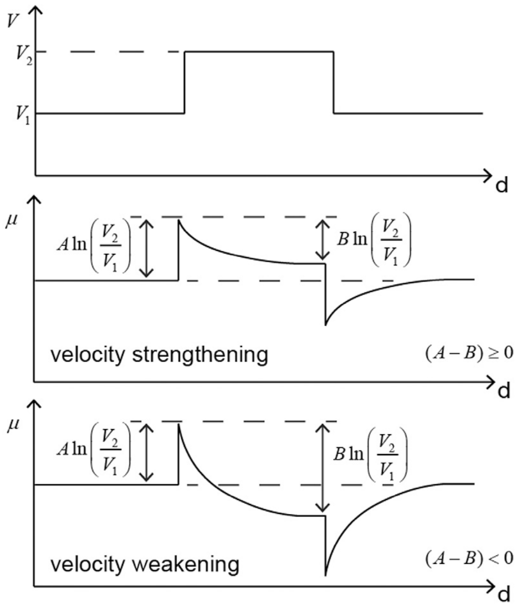

**Fig. 3.** Rate-and-state friction model [19,20]. Under the step change in sliding speed, friction shows a transient behavior similar to the complex fluid lubrication model. The stability of sliding is determined by the relationship between steady-state friction and sliding speed. Velocity strengthening gives stable sliding, and velocity weakening can cause instability in sliding such as stick–slip behaviors.

## 6. Discussion and conclusion

### 6.1. Rate-and-state friction model

Modeling friction using an evolution equation of a state variable is not a new idea in the literature. In geology, there have been many efforts to model transient friction responses as a function of state variables in order to explain the slip mechanics of earthquakes [18–22]. The models in the studies, which are widely called *rate-and-state friction models*, assume that the surface has a 'state' at any time, and the state is quantified using a state variable. The state variable represents the surface memory of previous siding. Therefore, under the same sliding history, reproducible results of friction are predicted [18]. Following is the equation form of the rate-and-state friction model [19,20]:

$$\tau=\sigma\left[\eta_0+A\ln\left(\frac{V}{V^*}\right)+B\ln\left(\frac{V^*\theta}{D_c}\right)\right] \tag{11}$$

$$\frac{d\theta}{dt}=-\frac{V}{D_c}\theta+1 \tag{12}$$

In Eq. (11), $\tau$ is a frictional stress, $\sigma$ is a normal stress, $V$ is a sliding speed, and $\theta$ is a state variable. $\eta_0$, $A$, and $B$ are parameters determined from experiments. The state variable $\theta$ is explained as a measure of contact population age, which is in close relation to growth of real contact area. When contact happens over time, the contact population age increases, and the real contact area increases together. The increasing real contact area causes increasing sliding resistance.

The time evolution behavior of $\theta$ is described by Eq. (12). The form of Eq. (12) is quite similar to the structure equation of complex fluid lubrication shown in Eq. (2). Eq. (12) has two competing terms on the right side and the decreasing rate is proportional to the sliding speed as well as the state variable.

The model predicts nearly identical behavior to that of complex fluid lubrication (Fig. 3). With a single step increase of sliding speed, there is an immediate jump in friction followed by decay, and vice versa for a single step decrease of sliding speed [19,20]. A difference in the models is that the rate-and-state model describes the behavior with respect to the sliding distance instead of the duration of sliding.

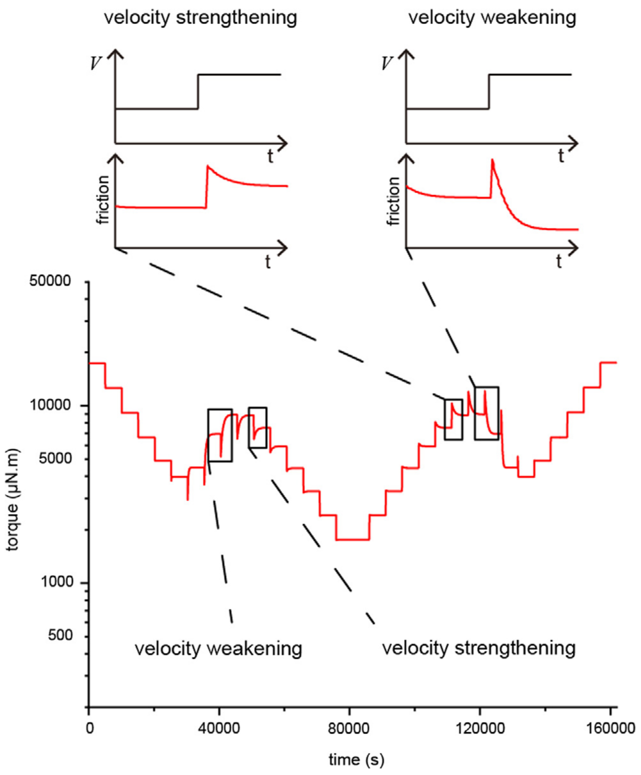

**Fig. 4.** The steady-state response of the complex fluid lubrication model includes both the velocity strengthening and weakening behaviors depending on the sliding speed.

The steady-state friction is an important parameter that determines the stability of the sliding. If the steady-state friction value increases at higher sliding speed, or $d\tau_{ss}/dV \geq 0$, the behavior is called 'velocity strengthening' and is considered stable response. If the steady-state friction value decreases at higher sliding speed, or $d\tau_{ss}/dV < 0$, the behavior is called 'velocity weakening' and is a condition for unstable response such as stick slip behavior or oscillation of friction depending on the stiffness of the system [18]. In the specific model described by Eqs. (11) and (12), the sign of $(A–B)$ determines the stability of the sliding.

The complex fluid model can also predict velocity strengthening and weakening behaviors. In the frictional torque-time graph in Fig. 4, the medium speed regime shows both velocity strengthening and weakening behavior depending on the sliding speed. One difference is that the rate-and-state model predicts only one behavior: either velocity strengthening or weakening for the same surface. The complex fluid model captures both behaviors depending on the sliding speed.

When a monotonic behavior either velocity strengthening or velocity weakening is analyzed, the rate-and-state model is more appropriate since we can reduce the number of parameters for model fitting. However, it cannot be applied to more complicated responses like hydrogel lubrication curves, and the complex fluid lubrication model is needed. Since the complex fluid lubrication model can describe all the features of the rate-and-state friction model as well as more complicated responses like local extrema, the complex fluid lubrication model can be considered a more general case of the rate-and-state model. When the complex fluid lubrication model is applied to the hard and dry surface sliding, no physical meaning of fluid flow is applicable, but the functional form can be used to describe the empirical trend.

The instability at the velocity weakening regime ($d\tau_{ss}/dV < 0$) is reported in a recent hydrogel friction study [3]. The study uses atomic force microscopy (AFM) for the friction test, which is an extremely compliant system. The stick–slip behavior is found in the regime where the friction decreases with sliding speed, which is an instability caused by the velocity weakening response.

### 6.2. Possible mechanism of the hydrogel lubrication

The state variable in rate-and-state friction model has the meaning of "age of contact", which represents the time-varying population of contact asperities [19]. This earthquake friction model exhibits similar concepts to thixotropy. The contacting population grows with time at slower speeds, which increases friction; conversely, the asperity contact population decreases at faster speeds, which decreases friction.

The surface adhesion was previously modeled as a source of hydrogel friction in the adsorption model by Gong [1], only considering the steady-state response of adhesion. In a more recent study, transient behavior of adhesion and friction depending on contact duration between the hydrogel surface and hard surface was reported [4]. The adhesion and friction increase with contact time when there is water drainage. Therefore, we can postulate that the water movement drives the change in the surface interaction, or adhesion.

Combining the concept of age of contact and adhesion change driven by water, we draw a schematic of the physical meaning of the complex fluid lubrication model (Fig. 5). The amount of water at the interface determines the degree of the direct contact between the polymer surface and hard surface. When faster sliding causes the water lubrication, this makes the surface abundant with water that prevents the direct contact, which decrease the adhesion and friction. When the water drainage occurs at the interface due to compression, the real contact area grows, which increases the macroscopic adhesion. Therefore, the source of the transient friction could be the transient surface adhesion due to the degree of intervention of water.

One important note about the water at the real contact area is that even when the direct contact occurs and water drains out from the interface, water always exists, not at the interface, but in the subsurface of the hydrogel. This remaining water still affects the frictional behavior of hydrogel, and the effect is included in Eq. (1) as the constant water viscosity that is always added to the frictional response.

The water drainage mechanism gives a physical meeting to each term in structural equation shown in Eq. (2). The first term on the right side represents the decreasing rate of the surface interaction due to the water. Since the amount of water coming to the interface depends on the sliding speed, the term is proportional to the sliding speed. Furthermore, if there is a lot of adsorption exist at a given time, there is more chance of desorption, so the decreasing rate includes $\lambda$ in it. The second term on the right side serves as the increasing rate of surface interaction. It is independent of speed and only dependent on the amount of vacant adsorption site at a time point of observation, which is expressed as $(1-\lambda)$.

Using this physical interpretation, we can discuss the physical picture of the lubrication hysteresis of hydrogels. When the sliding speed decreases from the hydrodynamic regime, contact area starts to grow over time, which makes the transient frictional response. If the friction is captured in the middle of the transient process due to the sliding time less than steady-state time scale, the real contact area is not fully increased or decreased at each sliding step, and the state of the contact area affects the next sliding step at a different speed. This generates the lubrication hysteresis. If the sliding time at each speed, or step time, is long enough to reach the steady state, contact area converges to specific value under the balance between increasing rate and decreasing rate.

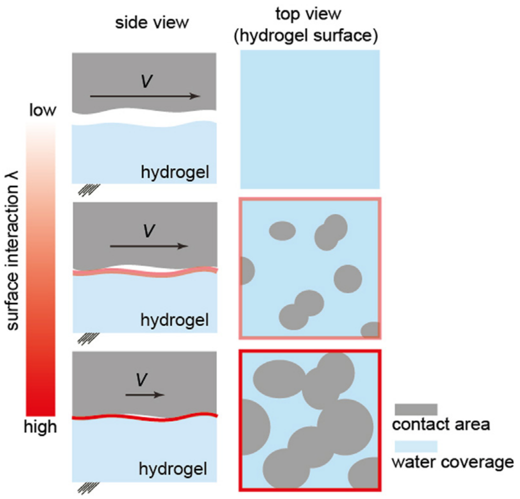

**Fig. 5.** The schematic of the physical mechanism of the complex fluid lubrication model. Water remaining at the interface prevents the direct contact and adhesion between the hydrogel and hard surfaces. As water drainage at the interface occurs at lower speeds, the direct contact area increases, and the macroscopic adhesion increases together. This induces a state of greater structure at lower speeds.

The physical picture of the steady state lubrication is similar to the well-known Stribeck curve for hard surface lubrication, with the exception of the low-speed regime. During low-speed sliding, the friction increases with sliding speed instead of high and relatively constant friction shown in the boundary lubrication regime of Stribeck curve. The positive slope, or velocity strengthening, that resembles the viscous flow can be caused by the elastic deformation of adsorbed polymers and its average bonding time, which is extensively described by Gong in her adsorption model [1]. The transition to negative slope, or velocity weakening, in the medium-speed regime is caused by water lubrication, and it is similar to the case of the mixed lubrication regime of Stribeck curve. The transition is also discussed in the adsorption model, but action of water is not considered as the source of this transition. The high-speed regime of complex fluid lubrication model corresponds to the hydrodynamic lubrication regime.

## Declaration of competing interest

The authors declare that they have no known competing financial interests or personal relationships that could have appeared to influence the work reported in this paper.

## Acknowledgments

The authors are grateful for helpful conversations and resources from Randy Ewoldt, Jonathon Schuh, and Anthony Margotta. This work was supported in part by NSF, United States of America Award #1751945.

## References

[1] J. Gong, Y. Osada, Gel friction: A model based on surface repulsion and adsorption, J. Chem. Phys. 109 (1998) 8062–8068, http://dx.doi.org/10.1063/1.477453.

[2] A.A. Pitenis, J.M. Urueña, K.D. Schulze, R.M. Nixon, a.C. Dunn, B.a. Krick, W.G. Sawyer, T.E. Angelini, Polymer fluctuation lubrication in hydrogel gemini interfaces, Soft Matter 10 (2014) 8955–8962, http://dx.doi.org/10.1039/C4SM01728E.

[3] T. Shoaib, J. Heintz, J.A. Lopez-Berganza, R. Muro-Barrios, S.A. Egner, R.M. Espinosa-Marzal, Stick-slip friction reveals hydrogel lubrication mechanisms, Langmuir 34 (2018) 756–765, http://dx.doi.org/10.1021/acs.langmuir.7b02834.

[4] E.R. Reale, A.C. Dunn, Poroelasticity-driven lubrication in hydrogel interfaces, Soft Matter 13 (2016) 428–435, http://dx.doi.org/10.1039/C6SM02111E.

[5] N.L. Cuccia, S. Pothineni, B. Wu, J. Méndez-Harper, J.C. Burton, Pore-size dependence and slow relaxation of hydrogel friction on smooth surfaces, 2020, http://arxiv.org/abs/2001.00620.

[6] J.M. Urueña, A.A. Pitenis, R.M. Nixon, K.D. Schulze, T.E. Angelini, W. Gregory Sawyer, Mesh size control of polymer fluctuation lubrication in gemini hydrogels, Biotribology 1–2 (2015) 24–29, http://dx.doi.org/10.1016/j.biotri.2015.03.001.

[7] G. Kagata, J.P. Gong, Y. Osada, Friction of gels. 6. Effects of sliding velocity and viscoelastic responses of the network, J. Phys. Chem. B 106 (2002) 4596–4601, http://dx.doi.org/10.1021/jp012380w.

[8] T. Kurokawa, T. Tominaga, Y. Katsuyama, R. Kuwabara, H. Furukawa, Y. Osada, J.P. Gong, Elastic-hydrodynamic transition of gel friction, Langmuir 21 (2005) 8643–8648, http://dx.doi.org/10.1021/la050635h.

[9] J.P. Gong, Friction and lubrication of hydrogels?its richness and complexity, Soft Matter 2 (2006) 544, http://dx.doi.org/10.1039/b603209p.

[10] A. Schallamach, A theory of dynamic rubber friction, Rubber Chem. Technol. 39 (1966) 320–327, http://dx.doi.org/10.5254/1.3544844.

[11] J. Kim, A.C. Dunn, Soft hydrated sliding interfaces as complex fluids, Soft Matter 12 (2016) 6536–6546, http://dx.doi.org/10.1039/C6SM00623J.

[12] J. Kim, A.C. Dunn, Thixotropic mechanics in soft hydrated sliding interfaces, Tribol. Lett. 66 (2018) 102, http://dx.doi.org/10.1007/s11249-018-1056-4.

[13] B.J. Hamrock, D. Dowson, Elastohydrodynamic lubrication of elliptical contacts for materials of low elastic modulus, Am. Soc. Mech. Eng. 100 (1978).

[14] A.C. Rennie, P.L. Dickrell, W.G. Sawyer, Friction coefficient of soft contact lenses: Measurements and modeling, Tribol. Lett. 18 (2005) 499–504, http://dx.doi.org/10.1007/s11249-005-3610-0.

[15] R. Simič, C.H. Mathis, N.D. Spencer, A two-step method for rate-dependent nano-indentation of hydrogels, Polym. (U. K.) 137 (2018) 276–282, http://dx.doi.org/10.1016/j.polymer.2018.01.017.

[16] A.A. Pitenis, W.G. Sawyer, Lubricity of high water content aqueous gels, Tribol. Lett. 66 (2018) 1–7, http://dx.doi.org/10.1007/s11249-018-1063-5.

[17] T. Shoaib, R.M. Espinosa-Marzal, Insight into the viscous and adhesive contributions to hydrogel friction, Tribol. Lett. 66 (2018) 1–14, http://dx.doi.org/10.1007/s11249-018-1045-7.

[18] A. Ruina, Slip instability and state variable friction laws, J. Geophys. Res. 88 (1983) 10359–10370, http://dx.doi.org/10.1029/JB088iB12p10359.

[19] J.H. Dieterich, B.D. Kilgore, Direct observation of frictional contacts: New insights for state-dependent properties, Pure Appl. Geophys. PAGEOPH 143 (1994) 283–302, http://dx.doi.org/10.1007/BF00874332.

[20] C.H. Scholz, Earthquakes and friction laws, Nature 391 (1998) 37–42, http://dx.doi.org/10.1038/34097.

[21] J.R. Rice, N. Lapusta, K. Ranjith, Rate and state dependent friction and the stability of sliding between elastically deformable solids, J. Mech. Phys. Solids 49 (2001) 1865–1898, http://dx.doi.org/10.1016/S0022-5096(01)00042-4.

[22] A. Helmstetter, B.E. Shaw, Afterslip and aftershocks in the rate-and-state friction law, J. Geophys. Res. Solid Earth 114 (2009) http://dx.doi.org/10.1029/2007JB005077.